Molecular Therapy
Methods & Clinical Development
Original Article

Sustained Correction of a Murine Model of Phenylketonuria following a Single Intravenous Administration of AAVHSC15-PAH

Seemin S. Ahmed,[1] Hillard Rubin,[1] Minglun Wang,[1] Deiby Faulkner,[2] Arnold Sengooba,[2] Serena N. Dollive,[1] Nancy Avila,[2] Jeff L. Ellsworth,[1] Diana Lamppu,[3] Maria Lobikin,[4] Jason Lotterhand,[2] Laura Adamson-Small,[4] Teresa Wright,[5] Albert Seymour,[1] and Omar L. Francone[1]

[1]Research and Development, Homology Medicines, 1 Patriots Park, Bedford, MA 01730, USA; [2]*In Vivo* Group, Homology Medicines, 1 Patriots Park, Bedford, MA 01730, USA; [3]Program Management Group, Homology Medicines, 1 Patriots Park, Bedford, MA 01730, USA; [4]Process Development, Homology Medicines, 1 Patriots Park, Bedford, MA 01730, USA; [5]Toxicology Group, Homology Medicines, 1 Patriots Park, Bedford, MA 01730, USA

Phenylketonuria is an inborn error of metabolism caused by loss of function of the liver-expressed enzyme phenylalanine hydroxylase and is characterized by elevated systemic phenylalanine levels that are neurotoxic. Current therapies do not address the underlying genetic disease or restore the natural metabolic pathway resulting in the conversion of phenylalanine to tyrosine. A family of hepatotropic clade F adeno-associated viruses (AAVs) was isolated from human CD34$^+$ hematopoietic stem cells (HSCs) and one (AAVHSC15) was utilized to deliver a vector to correct the phenylketonuria phenotype in Pah^{enu2} mice. The AAVHSC15 vector containing a codon-optimized form of the human phenylalanine hydroxylase cDNA was administered as a single intravenous dose to Pah^{enu2} mice maintained on a phenylalanine-containing normal chow diet. Optimization of the transgene resulted in a vector that produced a sustained reduction in serum phenylalanine and normalized tyrosine levels for the lifespan of Pah^{enu2} mice. Brain levels of phenylalanine and the downstream serotonin metabolite 5-hydroxyindoleacetic acid were restored. In addition, the coat color of treated mice darkened following treatment, indicating restoration of the phenylalanine metabolic pathway. Taken together, these data support the potential of an AAVHSC15-based gene therapy as an investigational therapeutic for phenylketonuria patients.

INTRODUCTION

Phenylketonuria (PKU) is a genetic disorder of liver metabolism that arises primarily from loss of function of the hepatic enzyme phenylalanine (Phe) hydroxylase (PAH), which is caused by mutations in the *PAH* gene. In the presence of a co-factor, tetrahydrobiopterin (BH_4), PAH hydroxylates Phe to produce tyrosine (Tyr) and subsequently dopamine, adrenaline, and melanin.[1] Lack of functional PAH results in hyperphenylalaninemia (HPA) after dietary intake of protein, causing elevated systemic Phe levels. HPA also causes a neurometabolic phenotype accompanied by cognitive impairment and behavior problems in patients on uncontrolled diets.[2,3] PAH deficiency manifests as a continuum of HPA phenotypes from mild HPA (blood Phe from 120 to 360 μmol/L) to severe, termed as classical PKU, which is the most common form and clinically defined as blood Phe levels exceeding 1,200 μmol/L. If left untreated, classical PKU results in progressive, irreversible neurological impairment during infancy and early childhood. Classical PKU patients have neurocognitive issues even when they are on a controlled, Phe-restricted diet after adolescence.[4] The disease shows multiple characteristics such as hypopigmentation in skin, hair, and eyes; eczema; growth retardation; and a mousy odor caused by accumulation of phenylacetate and phenyllactate.[5] There are more than 950 known mutations in the *PAH* gene, with the vast majority being missense mutations.[2] Although recessively inherited mutations in the *PAH* gene underlie most PKU cases, about 2% of the PKU patient population have a deficiency of the cofactor BH_4 that can be corrected by oral supplementation of the missing cofactor.[6] The cornerstone of current PKU therapy is restriction of Phe where dietary protein is replaced with a Phe-free liquid formula. The onerous diet makes it difficult to balance nutrients and eventually leads to lack of compliance,[7] with a serious impact on neurocognitive health. Additionally, the reduction of dietary Phe intake does not restore Tyr levels and subsequent neurotransmitter synthesis. Introduction of functional PAH by gene therapy has the potential to correct the deficiency in the metabolic pathway by addressing the underlying genetic defect and provide a lasting effect following a single dose.

The most widely used murine model of PKU, the homozygous Pah^{enu2} mouse, has a point mutation in exon 7 (c.835T>C; p.F263S) resulting in approximately 1% of wild-type (WT) hepatic PAH activity.[8] Blood Phe levels are increased 15- to 20-fold, and hypopigmentation is observed due to reduced melanin production, which manifests as lighter color fur.[8] These features recapitulate classical PKU in humans, making this a valid model to evaluate the

Received 4 February 2020; accepted 10 March 2020;
https://doi.org/10.1016/j.omtm.2020.03.009.

Correspondence: Omar L. Francone, Research and Development, Homology Medicines, 1 Patriots Park, Bedford, MA 01730, USA.
E-mail: ofrancone@homologymedicines.com

therapeutic potential of gene therapy approaches for the treatment of PKU.

Early research has shown that liver-mediated gene therapy using an adenovirus vector transiently reverses HPA in Pah^{enu2} mice, but efficacy was lost due to an immune response to the adenoviral capsid.[9] Alternatively, adeno-associated viruses (AAVs) are non-pathogenic viruses of lower immunogenicity that can mediate long-term episomal transgene expression in non-dividing or slowly dividing cells.[10] *PAH* gene therapy using AAVs has been attempted in mice by a number of groups using different routes of administration, AAV serotypes, or vector designs.[5,11–13] More recently, Yagi et al.[14] have reported that the intraperitoneal administration of a self-complementary AAV8 expressing murine PAH under the control of a liver-specific promoter to Pah^{enu2} led to a reduction of serum Phe to normal or near-normal levels up to a year following administration. No published report has demonstrated sustained correction in a murine model of PKU following a single intravenous (i.v.) administration of human *PAH* at low doses of viral vectors.

In the studies described herein several vectors were screened and packaged in recombinant AAVHSC15, a clade F AAV isolated from human hematopoietic stem cells.[15] Two of the vectors tested reduced blood Phe within a week of administration and darkened coat color in Pah^{enu2} mice, a sign of restoration of melanin production. The administration of an AAVHSC15 containing a ubiquitous promoter (AAVHSC15-chicken β-actin [CBA]-PAH) rescued the high blood Phe phenotype within a week at a dose approximately a log lower than previously reported,[5,11–13] but the reduction of serum Phe was transient. Further optimization including the use of a liver-specific promoter and a codon-optimized human *PAH* cDNA resulted in a vector (AAVHSC15-PAH) designated HMI-102. A single i.v. dose of HMI-102 restored the underlying loss of function of PAH activity caused by mutations in the *PAH* gene, achieved a sustained reduction of serum Phe, and normalized serum Tyr levels for the lifespan of Pah^{enu2} mice at a 10-fold lower dose than AAVHSC15-CBA-PAH. In addition, brain levels of Phe and 5-hydroxyindoleacetic acid (5-HIAA) were restored. Taken together, these data support further development of AAVHSC15-PAH as an investigational gene therapy candidate for PKU.

RESULTS

Characterization of the Pah^{enu2} Mouse

The Pah^{enu2} mouse model has a homozygous missense mutation (F263S in exon 7) in the active site of *PAH*, resulting in 1% of WT activity.[8] Mutations in exon 7 are common in PKU patients in a compound heterozygous context.[16] Impaired Phe metabolism reduces production of Tyr and eumelanin and is responsible for hypopigmentation in Pah^{enu2} mice. Mutant Pah^{enu2} males are smaller and weigh less than WT males (29.5 ± 4.5 g compared to 38.3 ± 2.2 g; $p < 0.001$, Figure S1A).

The murine model has several features consistent with the classical PKU phenotype, notably high blood Phe levels compared to the parent strain (1,458 ± 378 μM as opposed to 92.6 ± 37.6 μM; $p < 0.0001$) when maintained on a Phe-containing normal chow diet. Tyr levels show an inverse trend with lower levels in mutant mice (21.3 ± 5.7 μM as opposed to 83.5 ± 34.6 μM; $p < 0.0001$). The average lifespan of male Pah^{enu2} mice was 235.5 days and that of female Pah^{enu2} mice was 157 days on a normal chow diet (Figure S1B). This is consistent with literature reports indicating that the background strain (BTBR) for the Pah^{enu2} mouse has a reduced lifespan compared to other mouse strains such as C57BL/6J.[17]

AAVHSC15-CBA-PAH Administration Corrected the PKU Phenotype *In Vivo*

The vector containing the human *PAH* cDNA flanked by the CBA promoter and the SV40 polyadenylation sequence was packaged into AAVHSC15. The expression cassette was designated AAVHSC15-CBA-PAH. This capsid was chosen based on its hepatic tropism previously observed.[18,19] To assess whether AAVHSC15-CBA-PAH could restore Phe metabolism *in vivo*, groups of four male Pah^{enu2} mice were injected with a single i.v. dose of AAVHSC15-CBA-PAH at various dose levels, that is, 1.6×10^{11}, 5×10^{11}, 1.6×10^{12}, and 5×10^{12} vector genomes (VG)/mouse. Phe and Tyr levels were measured in blood collected immediately prior to dosing and then at weekly intervals for 4 weeks.

At all doses, injected mice showed a dose-dependent reduction in Phe levels and a concomitant increase in Tyr levels in the blood within 1 week of vector administration (Figure 1A). Phe levels rebounded and Tyr levels declined in mice treated with the two lower doses of AAVHSC15-CBA-PAH (Figures 1A and 1B). Similar findings were observed in female Pah^{enu2} mice (data not shown).

A second study was performed using a group of six male mice dosed at 2×10^{12} VG/mouse with AAVHSC15-CBA-PAH to examine hepatic transduction, human *PAH* expression, and PAH enzyme activity. All mice treated with AAVHSC15-CBA-PAH showed darkened coat color (Figure 1C) and a reduction in serum Phe levels within 1 week of administration, which was sustained to the end of the 4-week study (Figure 1D). At study termination, VG levels were 1.2×10^6 VG/μg of DNA in the liver of treated mice (Figure 1E), indicating the high liver tropism of the AAVHSC15 capsid. The presence of human *PAH* VGs in the liver was associated with increases in human *PAH* mRNA (Figure 1F) and restoration of PAH enzyme activity to approximately 20% of the levels observed in WT mice (Figure 1G). These data are consistent with liver repopulation studies conducted in PKU-deficient mice by Hamman et al.[20] using hepatocytes from WT or heterozygous Pah mice demonstrating that blood Phe levels within the normal range were observed when approximately 10% of the hepatocytes expressed PAH.

Vector Optimization to Increase the Efficacy of AAVHSC15-Based Gene Therapy

Durability of expression and phenotypic correction are key criteria for a successful gene therapy approach. To evaluate whether expression of *PAH* was sustained, groups of five male Pah^{enu2} mice were dosed

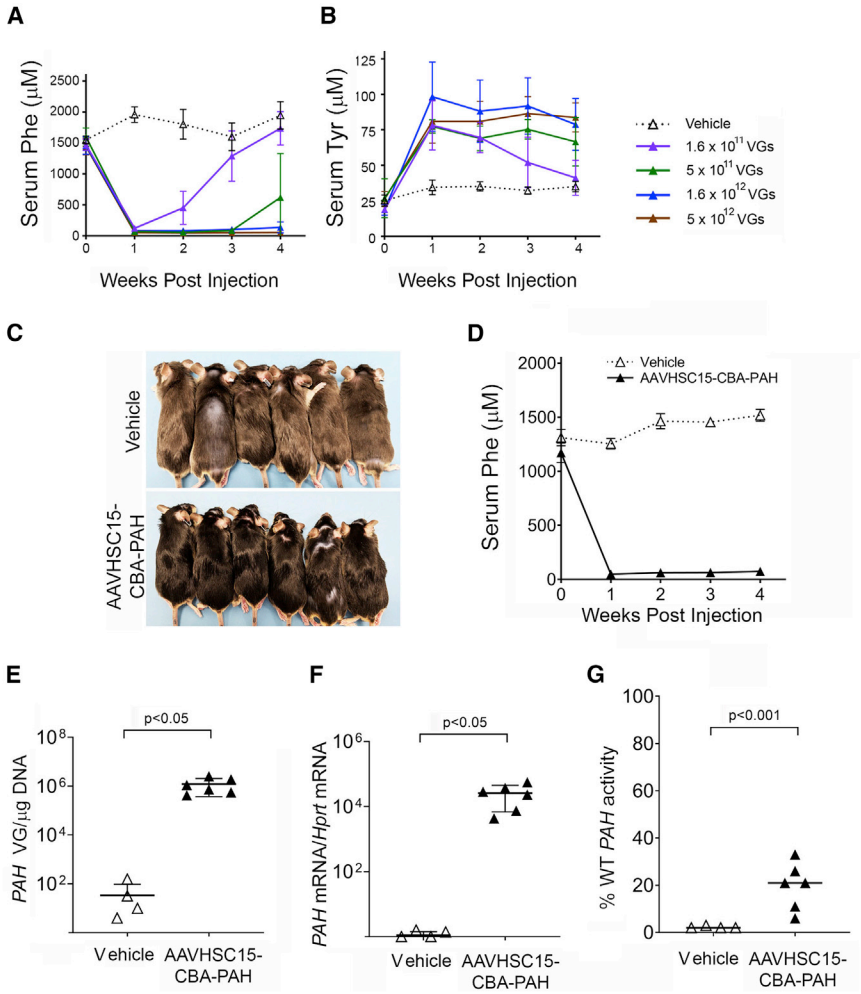

Figure 1. Treatment of Pah^{enu2} Mice with AAVHSC15-CBA-PAH

(A and B) Serum Phe (A) and serum Tyr (B) levels in 7-week-old male Pah^{enu2} mice following intravenous administration via tail vein injection of vehicle or AAVHSC15-CBA-PAH at various doses. Serum Phe and Tyr concentrations were determined weekly for the duration of the study as described in Materials and Methods. (C) Pigmentation phenotype correction observed in male Pah^{enu2} mice treated with AAVHSC15-CBA-PAH at 2 × 10^{12} VG/mouse. (D) Serum Phe levels in 7-week-old male Pah^{enu2} mice following intravenous administration of vehicle (n = 4) or 2 × 10^{12} VG/mouse of AAVHSC15-CBA-PAH (n = 6). (E) Vector genome concentrations in liver of Pah^{enu2} mice treated with vehicle or 2 × 10^{12} VG of AAVHSC15-CBA-PAH 4 weeks after administration. Vector genomes were determined from genomic DNA extracted from liver samples as described in Materials and Methods. (F) Liver human *PAH* and murine mRNA *Hprt* levels in Pah^{enu2} mice treated with vehicle (n = 4) or 2 × 10^{12} VG of AAVHSC15-CBA-PAH (n = 6) were determined 4 weeks after administration by qRT-PCR as described in Materials and Methods. Human *PAH* mRNA levels were normalized to the murine housekeeping *Hprt* mRNA levels and expressed as human *PAH* mRNA/*Hprt* mRNA. (G) Human *PAH* activity in vehicle and AAVHSC15-CBA-PAH-treated Pah^{enu2} mice 4 weeks after administration. PAH activity was determined in liver tissue homogenates by LC-MS/MS as described in Materials and Methods. PAH activity levels were expressed as the percentage of PAH activity levels measured in liver homogenates from wild-type mice. Data in (A)–(C) are represented as mean ± SD. Statistical significance between groups in (E)–(G) was determined by the Student's t test.

with AAVHSC15-CBA-PAH at 1.6 × 10^{12} and 5 × 10^{12} VG/mouse, the two higher doses tested previously. Both doses showed a reduction of Phe to normal levels (81.1 ± 32.5 μM; $p < 0.0001$) within 1 week (Figure 2A). The highest dose tested led to a sustained reduction in serum Phe for 12 weeks, the duration of the study (Figure 2A). Injected mice showed a dose-dependent accumulation of VGs and mRNA levels (Figures S2A and S2B). The absence of sustained reduction of serum Phe at the low doses tested prompted modifications in the construct design to increase the efficacy of the vector. Several new constructs, including changes in promoters and codon optimization, were made (Figure 2B). Codon optimization was used to identify a cDNA sequence for the human *PAH* gene that would exhibit elevated and durable levels of human *PAH* mRNA in mouse liver.

Two methods were used to optimize transgene expression: variation in the number of cytosine-guanosine (CpG) dinucleotides in the *PAH* cDNA and the codon adaptation index (CAI). The CAI indicates usage of highly expressing codons; that is, higher CAI values indicate higher estimated protein expression. Nevertheless, the higher CpG dinucleotide count within a construct increases the potential likelihood of silencing mediated by CpG methylation,[21] degradation of the VG mediated by TLR9 activation,[22] or degradation of RNA mediated by the zinc finger antiviral protein (ZAP).[23] Predicted CAI and CpG dinucleotide counts for each sequence obtained from the COOL program are shown in Figure 2C. An increase along the x axis indicates higher predicted protein expression. Constructs that had a lower CpG content but higher potential for durable expression compared to the unoptimized *PAH* sequence (Figure 2C) were selected for testing. Tested cDNAs were compared for relative identity and clustered together. The results are superimposed on a heatmap indicating relative identity between the algorithm-generated sequences (Figure 2D). Sequences selected for testing *in vivo* in Pah^{enu2} mice are indicated as closed diamonds and compared to the WT human *PAH* sequence (closed squares).

Single-stranded oligodeoxyribonucleotides that have a central CpG core can stimulate immune cells[24,25] and lead to silencing or clearance of the transduced hepatocytes and loss in efficacy. In order to test this

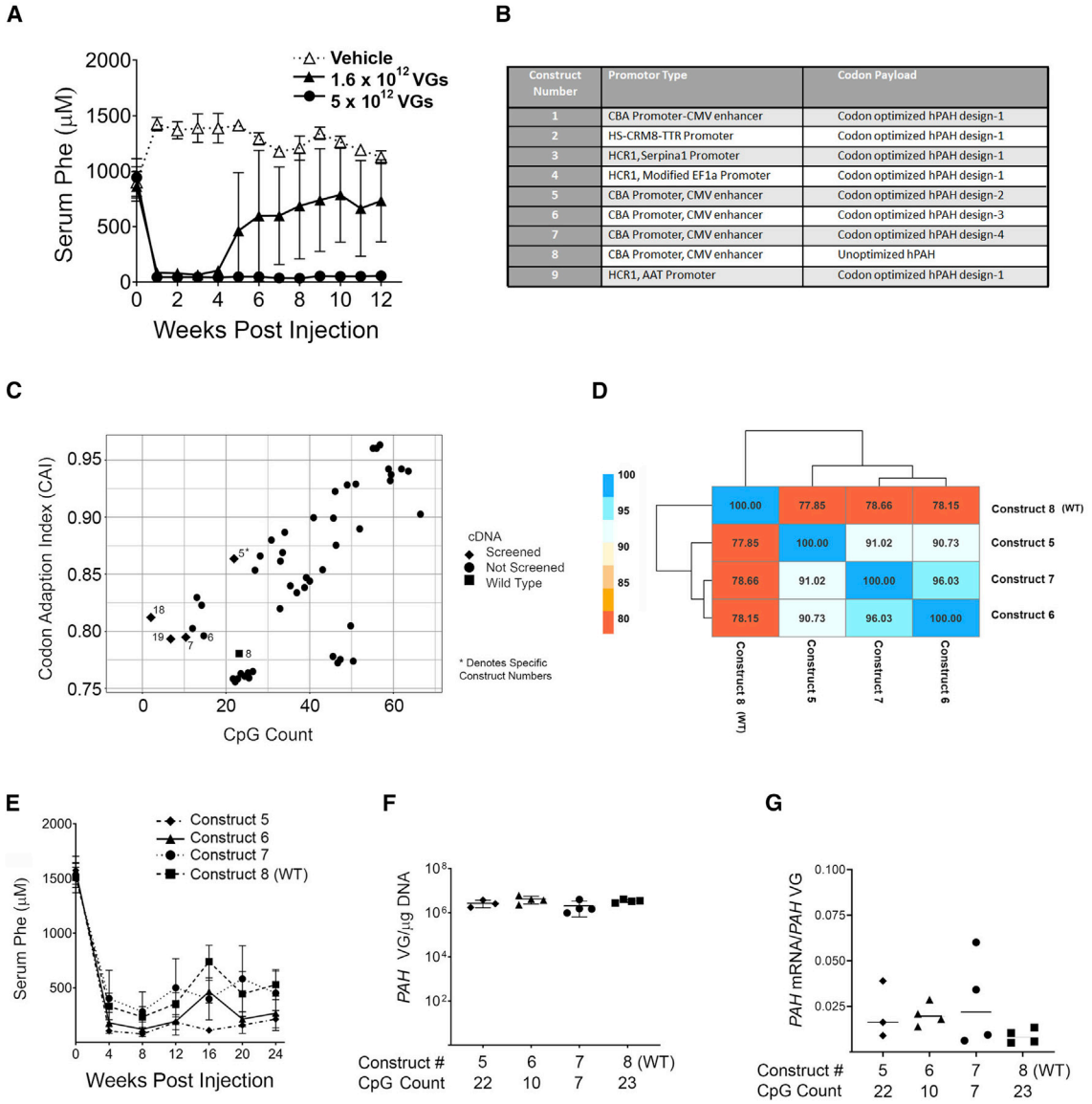

Construct Number	Promotor Type	Codon Payload
1	CBA Promoter-CMV enhancer	Codon optimized hPAH design-1
2	HS-CRM8-TTR Promoter	Codon optimized hPAH design-1
3	HCR1, Serpina1 Promoter	Codon optimized hPAH design-1
4	HCR1, Modified EF1a Promoter	Codon optimized hPAH design-1
5	CBA Promoter, CMV enhancer	Codon optimized hPAH design-2
6	CBA Promoter, CMV enhancer	Codon optimized hPAH design-3
7	CBA Promoter, CMV enhancer	Codon optimized hPAH design-4
8	CBA Promoter, CMV enhancer	Unoptimized hPAH
9	HCR1, AAT Promoter	Codon optimized hPAH design-1

Figure 2. AAVHSC15-CBA-PAH and Codon-Optimized AAVHSC15-CBA-PAH Versions Tested in Pah^{enu2} Mice

(A) Two doses of AAVHSC15-CBA-PAH (1.6×10^{12} and 5×10^{12} VG/mouse) were administered to 7-week-old Pah^{enu2} mice by single tail vein administration and compared to a vehicle-treated control group. Serum Phe levels were assessed weekly for the duration of the study as described in Materials and Methods. (B) List of constructs designed and tested. (C) Optimization of vector elements to yield new therapeutic vector designs. The human *PAH* gene was codon optimized bioinformatically to yield an aggregate of usable sequences that were ranked on the codon adaptation index (CAI) and CG count. The plot displays predicted expression (CAI) and CpG count for optimized sequence and the wild-type cDNA as calculated using the COOL program. Higher CAI values indicate higher predicted protein expression. (D) Tested cDNAs were compared for relative identity and clustered. The table displays pairwise sequence identity between each sequence and is superimposed over a heatmap indicating the same. Dendrogram displays relationship between cDNA and was calculated via hierarchical clustering. (E) Effect of codon optimization of the human *PAH* cDNA on serum Phe levels in Pah^{enu2} mice. Constructs 5 (◆), 6 (▲), 7 (●), and 8 (■) were administered at 2×10^{12} VG/mouse intravenously via the tail vein. Serum Phe concentrations were determined every 4 weeks for the duration of the study as described in Materials and Methods. (F) Levels of vector genomes in liver samples from Pah^{enu2} mice treated with the various codon-optimized human PAH vectors. Vector genomes were determined from genomic DNA extracted from liver samples as described in Materials and Methods. (G) Human *PAH* mRNA was determined in liver samples by qRT-PCR as described in Materials and Methods. Human *PAH* mRNA levels are expressed as a ratio of the amount of VGs presents in the same liver samples. Data for (A) and (E) are represented as mean ± SD.

hypothesis, a subset of vectors (namely constructs 5, 6, 7, and 8 containing 22, 10, 7, and 23 CpG counts, respectively) optimized for CpG counts in the human *PAH* cDNA sequence under the same promoter (CBA) were injected into the Pah^{enu2} mice (n = 4) and assayed for their ability to reduce serum Phe during 24 weeks post-injection (Figure 2E). No correlation between CpG content and efficacy was

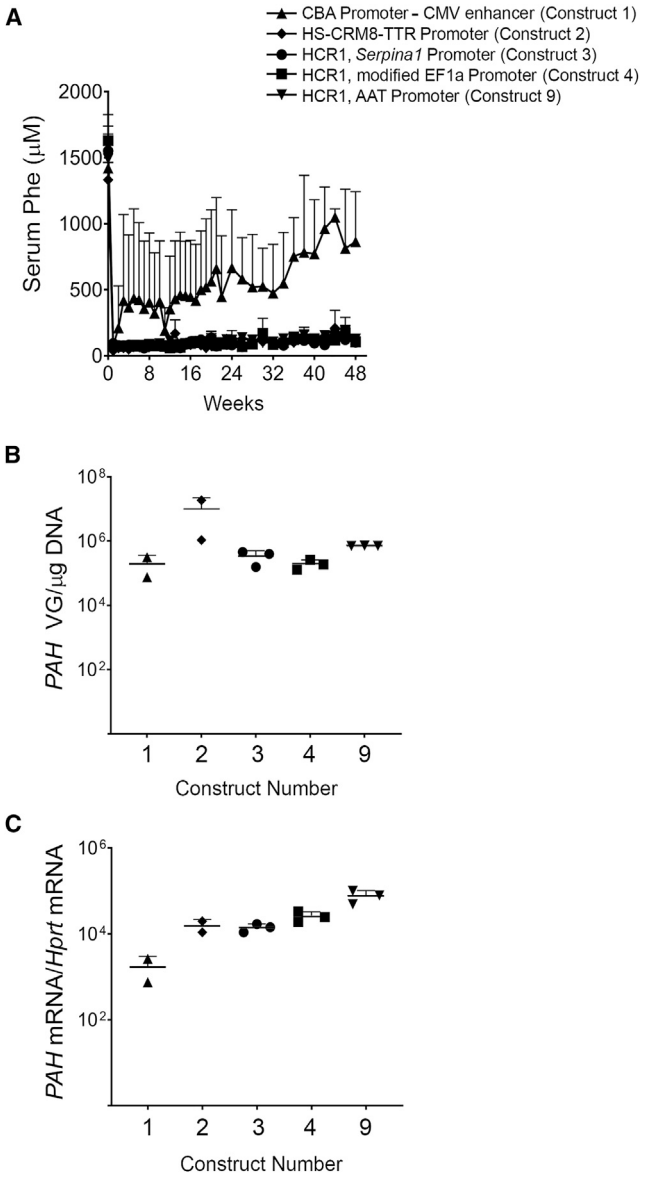

Figure 3. Optimization of AAVHSC15-CBA-PAH

(A) Male Pah^{enu2} mice were treated by single tail vein administration of AAVHSC15-CBA-PAH (construct 1) or four additional designs containing liver-specific promoters (constructs 2, 3, 4, and 9). Serum Phe levels were determined as described in Materials and Methods for the duration of the study. Data are represented as mean ± SD. (B) Liver VG levels for all constructs tested. Vector genome levels were determined as described in Materials and Methods. (C) Human *PAH* mRNA and murine *Hprt* levels were determined by RT-PCR as described in Materials and Methods.

observed. Construct 5 reduced and maintained serum Phe levels for the duration of the study while a loss of efficacy was observed with the unoptimized WT cDNA sequence vector (construct 8) despite having similar CpG counts of 22 and 23 CpG for constructs 5 and 8, respectively. Similarly, construct 7 (Figure 2E, closed circles) showed a rebound in blood Phe levels in spite of having three times lower CpG counts than construct 5. Construct 6 showed more sustained efficacy than construct 7 despite having more CpG counts of 10 and 7 CpG for constructs 6 and 7, respectively. Taken together, these findings indicate that the number of CpG counts in the *PAH* cDNA is not sufficient to explain the differences in efficacy observed in Pah^{enu2} mice. Similar hepatic VG levels were observed in all groups at the termination of the study (Figure 2F), indicating comparable hepatic transduction by all designs tested. The ratios of mRNA to VG were similar across different codon-optimized designs, further supporting the hypothesis that the CpG content within the human *PAH* cDNA does not affect the mRNA levels or efficacy of the tested constructs (Figure 2G).

We hypothesized that enhanced expression of the vector in the liver at lower doses may require a combination of a liver-specific promoter and a hepatotropic capsid. Thus, we developed chimeric promoters from combinations of the human apolipoprotein E/C-I hepatic control region enhancer (HCR1) and genes that express a large number of transcripts such as the alpha1 antitrypsin gene (SERPINA1) and the elongation factor 1 alpha (EF1α) to make three constructs: constructs 3, 4, and 9. A computationally derived chimeric promoter containing the hepatocyte-specific *cis*-regulatory module (HS-CRM8) was combined with the transthyretin (TTR) promoter to make construct 2.[26] Construct 1 contained CBA as a ubiquitous promoter and was used as a reference. All designs were generated by using the same codon-optimized version of the human *PAH* containing 22 CpG counts, packaged in AAVHSC15, and tested at a dose of 2×10^{12} VG/mouse. All vectors with liver-specific promoters normalized blood Phe levels in Pah^{enu2} mice within the first week of administration and sustained the phenotypic correction out to 48 weeks. In contrast, construct 1, containing the ubiquitous CBA promoter, showed a loss of efficacy over time (Figure 3A). In this study, constructs 2, 3, 4, and 9 containing liver-specific promoters were administered at a log-lower dose than the dose tested for construct 1. Liver concentrations of VGs did not differ significantly among all liver-specific promoter designs when compared to construct 1 (Figure 3B). Hepatic *PAH* mRNA levels were significantly higher (Figure 3C, $p < 0.01$) in Pah^{enu2} mice treated with AAVHSC15 vector containing liver-specific promoters (constructs 2, 3, 4, and 9) when compared to the AAVHSC15 vector design containing a ubiquitous CBA promoter (construct 1). Based on these findings, construct 9 was selected for further experiments.

Optimized Vector Efficiently Corrected PKU in Pah^{enu2} Mice

To assess the efficacy of the optimized vector AAVHSC15-PAH (construct 9), Pah^{enu2} male mice were dosed at 4×10^{11} VG/mouse (n = 4 per group), a dose 10-fold lower than that used for the non-optimized AAVHSC15-CBA-PAH vector. Treated mice showed darkened coat color (data not shown) and a reduction in serum Phe within 1 week of administration (Figure 4A) that persisted until the end of the study at 12 weeks. All cohorts of mice sacrificed at earlier time points showed the same kinetics on Phe lowering. Vector

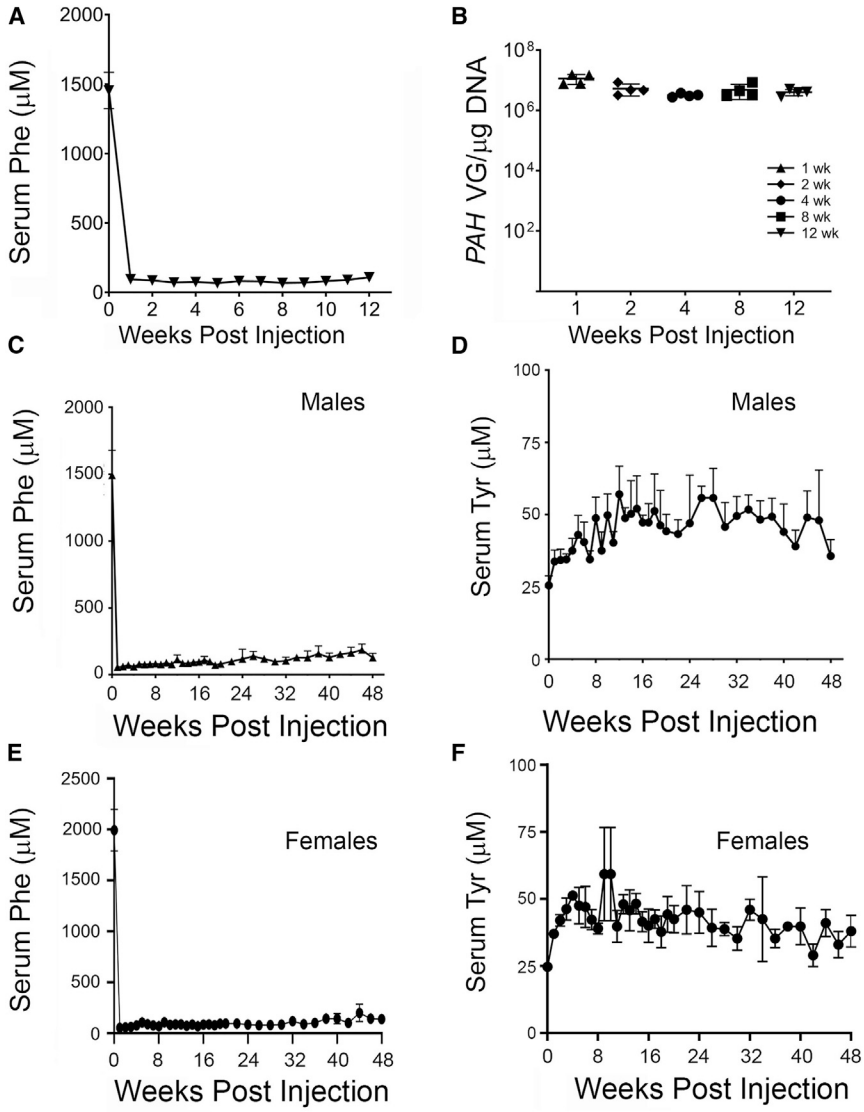

Figure 4. Efficacy of Optimized AAVHSC15-PAH Vector in Pah^{enu2} Mice

(A) Male Pah^{enu2} mice were administered a single intravenous dose of AAVHSC15-PAH via tail vein, and cohorts of four mice were sacrificed at 1, 2, 4, 8, and 12 weeks after administration. Serum Phe was determined as described in Materials and Methods. (B) Vector genomes levels in liver at 1, 2, 4, 8, and 12 weeks after administration of AACHSC15-PAH in male Pah^{enu2} mice. Vector genomes were determined as described in Materials and Methods and expressed as VG/μg of DNA. (C and D) Serum Phe (C) and Tyr (D) concentrations in male Pah^{enu2} mice were determined as described in Materials and Methods throughout the lifespan of male Pah^{enu2} mice. (E and F) Serum Phe (E) and Tyr (F) concentrations in female Pah^{enu2} mice were determined as described in Materials and Methods throughout the lifespan of female Pah^{enu2} mice. Data in (A), (C), and (D)–(F) are represented as mean ± SD.

genomes in livers declined from week 1 to week 2 after the dose and remained stable from 2 to 12 weeks (Figure 4B).

While this study was underway, a long-term single i.v. dose efficacy study with AAVHSC15-PAH was initiated in male and female Pah^{enu2} mice fed *ad libitum* a normal chow diet for the duration of the study. Serum Phe and Tyr levels were assessed for 48 weeks. The 48-week time point was chosen for terminal sacrifice, as it is consistent with the lifespan of the model. A single-dose i.v. administration of AAVHSC15-PAH at 4×10^{11} VG/mouse in males (Figure 4C) and 9×10^{11} VG/mouse in females (Figure 4E) reduced blood Phe concentrations to normal levels within 1 week following administration (55 ± 24 μM in males and 54 ± 4 μM in females). Mean serum Phe concentrations remained below 120 μM and consistent with normal levels during the course of the 48-week study in both male (mean, 101 ± 38 μM) and female (mean, 94 ± 38 μM) mice. A corresponding increase from baseline in Tyr concentration was also observed (Figures 4D and 4F; $p < 0.05$) in male and female Pah^{enu2} mice, indicating restoration of the Phe/Tyr metabolic pathway. Consistent with the reduced levels in serum Phe, vector genomes were detected in liver tissues at 48 weeks ($2.1 \times 10^6 \pm 4 \times 10^4$ VG/μg of DNA and $3.4 \times 10^6 \pm 7.9 \times 10^5$ VG/μg of DNA for male and female Pah^{enu2} mice, respectively).

The effect of AAVHSC15-PAH in the metabolism of Phe and related metabolites in the brain was also examined. The serotonin metabolite 5-HIAA (Figure 5A), a pharmacodynamic marker for PKU patients,[27] is significantly decreased in Pah^{enu2} mice when compared to WT parental mice (Figure 5B, $p < 0.001$), suggesting that the Pah^{enu2} mice reflect neurotransmitter deficits observed in PKU patients.[28] Treatment with AAVHSC15-PAH was associated with increases in levels of 5-HIAA in brain, reaching levels comparable to those found in the parental strain at 4 weeks post-dose (Figure 5B). In addition, Phe levels in the brains of Pah^{enu2} mice were decreased to levels observed in WT mice 4 weeks following the administration of AAVHSC15-PAH (Figure 5C). Restauration of normal brain Phe levels and concomitant increases in brain 5-HIAA were also seen in female Pah^{enu2} mice (data not shown). These findings support the potential of a liver-mediated *PAH* gene therapy to address the elevated Phe levels observed in the brain tissue of PKU patients.[29]

AAVHSC15-PAH Restored Phe Levels in the PKU Mouse Model in a Dose-Dependent Manner

In order to determine the pharmacologically effective dose range of AAVHSC15-PAH, we conducted a dose-ranging efficacy study in

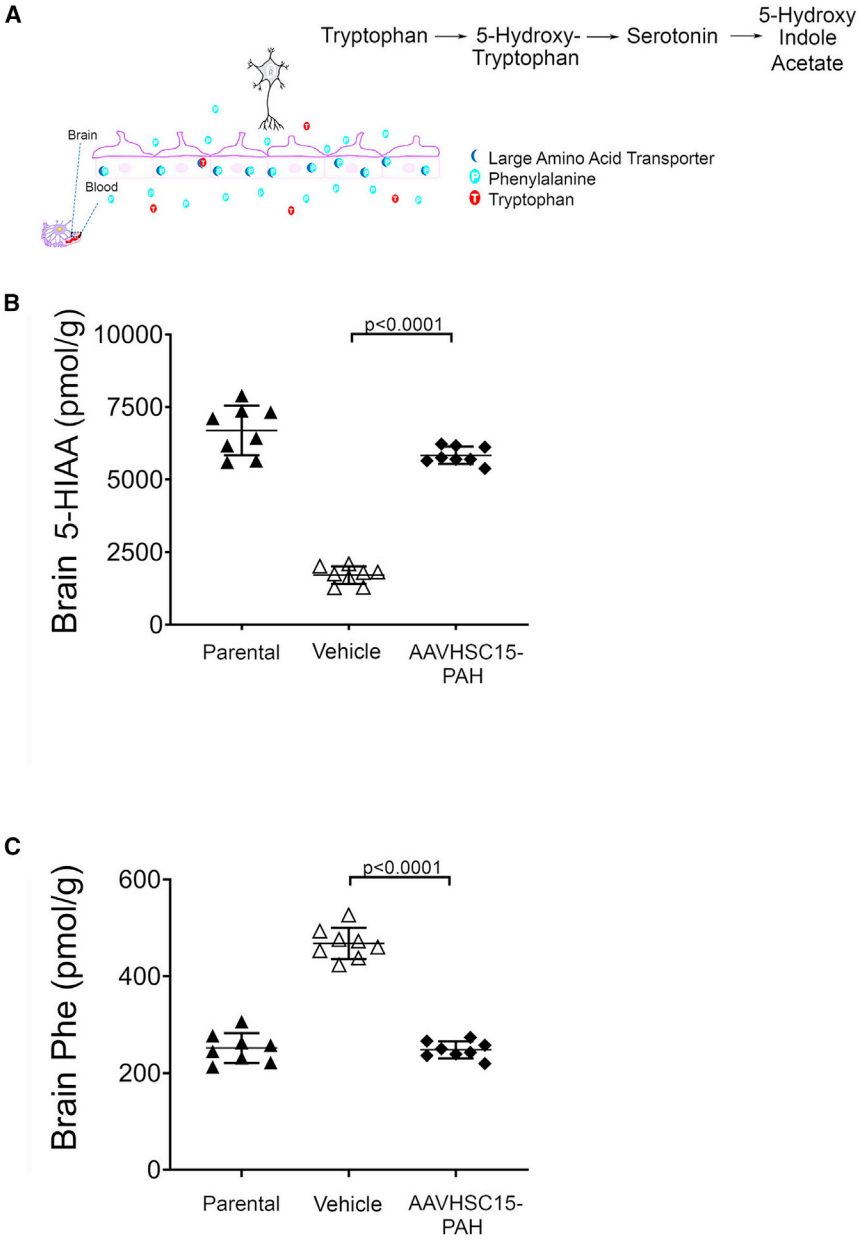

Figure 5. Restoration of Phe and 5-HIAA Levels in the Brain of Pah^{enu2} Mice

(A) Tryptophan metabolic pathway leading to the formation of 5-HIAA. (B) Brain levels of the serotonin metabolite 5-HIAA in vehicle or AAVHSC15-treated Pah^{enu2} mice and parental BTBR mice. Brain 5-HIAA levels were determined as described in Materials and Methods. (C) Brain Phe levels in the brain tissue of vehicle- or AAVHSC15-treated Pah^{enu2} and parental BTBR mice. Statistically significant differences were determined by the Students' t test. $p < 0.0001$, vehicle versus AAVHSC15-PAH treated PAH^{enu2} mice.

Pah^{enu2} mice. In this study, AAVHSC15-PAH was administered by a single i.v. injection via the tail vein at one of five doses over approximately a 1.5-log range. Mice were sacrificed 4 weeks after dosing. A dose-responsive decrease in blood Phe was observed over the course of the study, in both male and female mice. As shown in Figures 6A and 6B, after treatment with 2×10^{11} VG/mouse AAVHSC15-PAH, serum Phe levels in male mice were 127 ± 106 μM on day 8, as were those in female mice treated with 4×10^{11} VG/mouse (150 ± 144 μM). The group mean Phe concentrations for male mice treated with 4×10^{11}, 8×10^{11}, and 1.6×10^{12} VG/mouse and female mice treated with 8×10^{11} and 1.6×10^{12} VG/mouse were below 120 μM at all intervals and maintained for the duration of the study. A corresponding increase in serum Tyr was observed relative to baseline and vehicle control in all mice at all doses evaluated (Figures 6C and 6D). As shown in Figure 6B, female Pah^{enu2} mice had an approximately 34% higher level of serum Phe at baseline than that in males (1,400 ± 95 μM and 1,048 ± 108 μM, respectively. At lower doses (1×10^{11} and 2×10^{11} VG/mouse), female mice showed higher levels of blood Phe following treatment with AAVHSC15-PAH when compared to male Pah^{enu2} mice.

Analysis of liver samples was also performed to assess the level of vector genomes 28 days following administration of AAVHSC15-PAH (Figures 7A and 7B). All mice treated with AAVHSC15-PAH had detectable levels of vector genomes. The levels increased in both male and female mice with each increasing dose level. Notable differences between male and female mice in the levels of AAVHSC15-PAH vector genomes were observed. The levels of vector genomes in the male mice were 1.7- to 3.2-fold higher when compared to female mice, consistent with the sex difference in AAV transduction previously reported in mice.[30] As with the vector genome results, the levels of expression increased with each dose level, and differences were noted between male and female mice (1.5- to 2.8-fold higher in males compared to females; data not shown).

Liver samples were also collected for *PAH* enzyme activity, and results are shown in Figures 7C and 7D. A dose-dependent increase in *PAH* activity was observed. At the highest dose tested (1.6×10^{12} VG/mouse), PAH activity was 98% ± 67% and 37% ± 11% of WT levels in males and females, respectively. Mean *PAH* activity was above 10% of WT levels at doses up to and above 2×10^{11} VG/mouse (16% ± 8%) in males and 4×10^{11} VG/mouse (12% ± 5%) in females 28 days following AAVHSC15-PAH administration and at sufficient levels to restore serum Phe to levels below 120 μM.

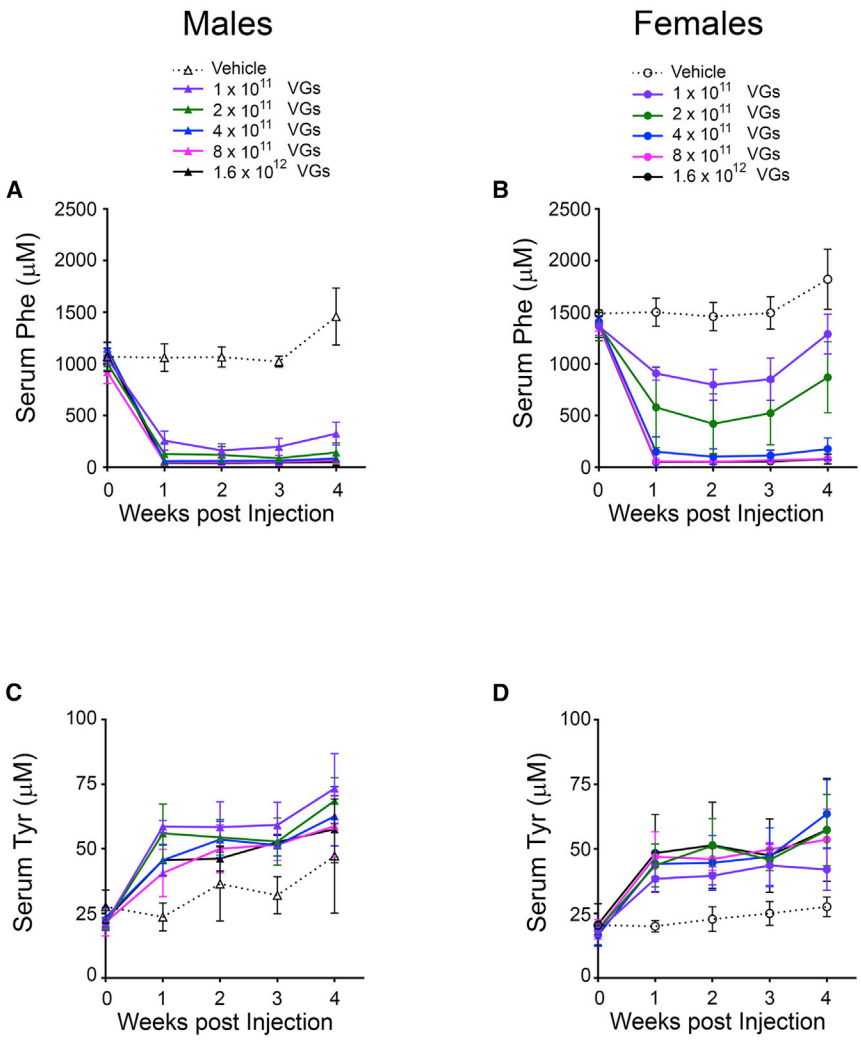

Figure 6. Dose Range Efficacy Study in Male and Female Pah^{enu2} Mice following Administration of AAVHSC15-PAH

(A–D) Serum Phe (A and B) and Tyr levels in male (A and C) and female (B and D) Pah^{enu2} mice following single tail vein injection of a range of doses of AAVHSC15-PAH (n = 5 mice/group) as described in Materials and Methods. Data in (A)–(D) are represented as mean ± SD.

DISCUSSION

PKU is an inborn error of Phe metabolism primarily caused by mutations in the *PAH* gene.[31] At present, a strict low-Phe diet is the standard of care for most PKU patients.[32] Compliance, however, is poor and such diets are also low in long-chain polyunsaturated fatty acids (LCPUFAs) and docosahexaenoic acid (DHA), both of which are important in neurological development.[33,34] Dietary Phe restriction does not address the underlying genetic deficiency of *PAH*, leading to the deficiency of Tyr and related downstream metabolites observed in patients with PKU. PKU patients have persistent white matter lesions, subtle neurologic changes, mood and behavior disturbances, and quality of life concerns even when their Phe intake is well controlled.[7,32,35,36]

Initial enzyme replacement studies with functional PAH did not prove effective for PKU.[37,38] Subcutaneous administration of an alternative enzyme that breaks down Phe in the blood, Phe ammonia lyase (PAL, EC 4.3.1.5), has shown effectiveness in reducing the blood concentration of Phe. PAL is an enzyme normally present in plants and fungi that deaminates Phe to ammonia and *trans*-cinnamic acid.[39] PAL reduces Phe within the blood but does not restore the affected biological pathway, including the synthesis of Tyr, a well-known neurotransmitter precursor. Current treatment strategies also include dietary restriction of Phe with or without augmentation of residual hepatic PAH activity by delivery of the BH_4 cofactor necessary to metabolize Phe.

In the present study, we showed that gene therapy has the potential to restore the underlying deficient biochemical pathway. Providing copies of the human *PAH* gene to produce functional enzyme would enable metabolism of Phe to its normal by-products and decrease its toxic accretion.

AAVs are potentially suitable gene therapy delivery vehicles given their tissue tropism and limited immunogenicity. Previous studies indicate that the presence of anti-AAV neutralizing antibodies, even at low titers, can block the transduction and compromise the effectiveness of AAV-based therapy in both preclinical and clinical studies.[10,40,41] Two of the AAVHSCs (AAVHSC15 and AAVHSC17) were tested against a panel of human sera samples and were shown to have a low seroprevalence of neutralizing antibodies.[18] Successful correction of PKU in the established PKU mouse model using recombinant AAVs (rAAVs) carrying *PAH* has been shown by several laboratories, although the therapy was less effective in female mice.[5,42] Similar sex-specific differences were observed in our studies consistent with literature reports.[30] Interestingly, enzyme substitution therapy using pegylated PAL,[43] which acts by a different mechanism than *PAH* gene replacement also showed lower efficacy in female Pah^{enu2} mice. Sex-based differences in transduction by AAVHSCs in non-human primates[18] or even sex-based differences in basal Phe levels of human patients[44] have not been reported, suggesting that the sex-based difference appears to be a characteristic specific to the PKU mouse model. Other than the sex-specific response to therapy, Pah^{enu2} mice recapitulate several symptoms of human patients with PKU and represent a well-established model to test the efficacy of investigational therapies for PKU.

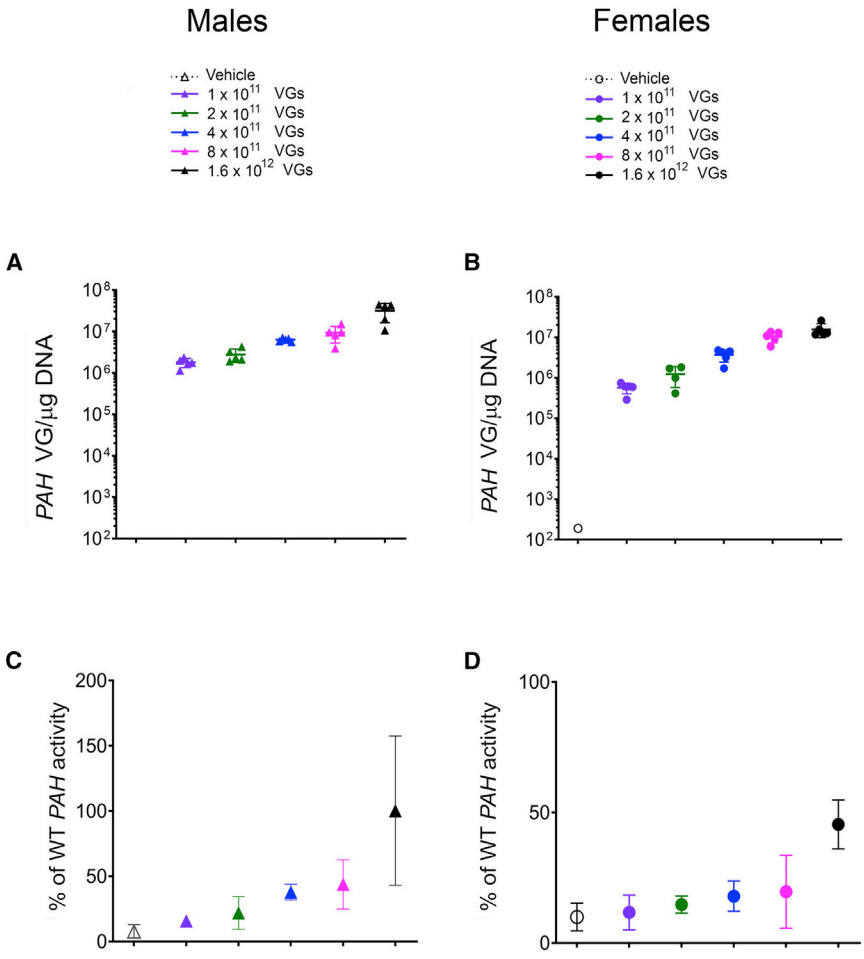

Figure 7. Vector Genomes and PAH Enzyme Activity in Male and Female Pah^{enu2} Mice following Administration of AAVHSC15-PAH

(A and B) Liver VG concentrations in males (A) and females (B) at all doses tested in the dose range efficacy study were determined following the protocol described in Materials and Methods. (C and D) *PAH* activity levels in males (C) and females (D) were determined from liver homogenates as described in Materials and Methods and expressed as percentage of the PAH activity measured in the wild-type BTBR parental strain. Data in (C) and (D) are expressed as mean ± SD.

Effectiveness of a gene therapy vector is a function of delivery to the target tissue, efficacy of the expression cassette, and durability of effect. We pursued a multipronged approach to develop an AAV-based therapy for PKU by combining a hepatotropic capsid with the human *PAH* gene and liver-restricted expression.[45–48] This combination allowed for lowering the vector dose while achieving long-term and sustained efficacy in the murine model.

Construct 1, the vector containing the ubiquitous promoter (AAVHSC15-CBA-PAH), restored clinically relevant levels of PAH enzyme activity that were accompanied by the normalized blood Phe levels in Pah^{enu2} mice within the first week of administration. Normalization of blood Phe levels was transient despite the presence of high levels of vector genomes in the liver, suggesting that the loss of efficacy was not due to poor transduction but rather low levels of *PAH* mRNA and, consequently, insufficient levels of PAH activity. Optimization of CpG dinucleotide repeats within the *PAH* sequence to address potential immune-related loss of transduced cells and efficacy[49,50] was unsuccessful in restoring long-term efficacy.

As demonstrated in studies on mouse models for Pompe disease and GSD1b, promoter specificity can determine the efficacy of a given vector design by restricting the transgene expression to the intended tissue,[51–53] avoiding cytotoxic T lymphocyte (CTL)-mediated toxicity and resulting in the clearance of the transduced cells and loss in therapeutic effects.[54] We tested several liver-specific promoters on a side-by-side comparison between AAVHSC15 vectors containing ubiquitous or liver-specific promoters and demonstrated a significant difference in hepatic mRNA levels consistent with the hypothesis that promoter specificity improves the efficacy of the therapeutic cassette.

The PKU mice developed by Shedlovsky et al.[8] (Pah^{enu2}/BTBR) survive for approximately 60 weeks in our laboratory; thus, all long-term studies were carried out until 48 weeks post-injection since mice were injected as adults at 7 weeks of age. In the studies described herein, several vectors demonstrated potential in delivering the human *PAH* gene at levels sufficient to restore PAH enzyme activity for the lifespan of the Pah^{enu2} mice even in the presence of a consistent and normal influx of Phe from the diet.

In conclusion, this work describes the identification of an investigational gene therapy for PKU designated HMI-102 based on a novel optimized AAVHSC15 that was isolated from human CD34$^+$ hematopoietic stem cells and injected i.v. to deliver a corrected copy of human *PAH*. Taken together, the findings from these studies demonstrate that liver-restricted expression of a codon-optimized version of human *PAH* resulted in the persistence of VGs in the liver accompanied by durable hepatic expression of human *PAH* mRNA and PAH enzyme activity levels sufficient to restore the natural metabolic pathway throughout the lifespan of the Pah^{enu2} mouse model, as shown by the normalization of serum and brain Phe, Tyr, and 5-HIAA levels. Collectively, these data support the potential of a gene therapy approach for PKU that could reduce Phe to normal levels and substantially restore the natural biological pathway.

MATERIALS AND METHODS

Vector Design

ssAAV (single-stranded AAV)/CAG-hPAH (human PAH) plasmid was used to build the vector construct 1 with the *CBA* promoter: CMV immediate early enhancer and codon-optimized human *PAH* cDNA, followed by the SV40 early polyadenylation signal. Construct 1 was used to generate AAVHSC15-CBA-hPAH by cloning into a plasmid containing AAV2 inverted terminal repeats (ITRs).

The self-complementary AAV vector AAVHSC15-PAH (construct 9) was developed with a 2,093-bp synthetic double-stranded DNA (dsDNA) gBlock fragment (IDT) that was subsequently PCR amplified and joined to an AAV2 ITR-containing plasmid by Gibson Assembly. It included a hybrid liver-specific promoter, with a codon-optimized form of the *PAH* gene (NCBI GenBank: NM_000277.2), and an SV40 late polyadenylation signal. The promoter contained a hepatic control region (HCR1), the *SERPINA1* (AAT) promoter, and 5′ UTR. The total construct size was 2,356 bp.

Construct 2 contained the HS-CRM8-TTR promoter as previously described[55] (PMID: 30700722). Construct 3 contained HCR1, the *SERPINA1* promoter, and modified 5′ UTR from the construct described in Picanço-Castro et al.[56] Construct 4 contained the HCR1 enhancer combined with human EF1a promoter with a 104-bp truncation, derived from the pEFIRES-P-mCherry-HPos plasmid. All constructs had the same *PAH* cDNA sequence. Promoters for constructs 2 and 3 were synthesized as 424- and 1,191-bp dsDNA gBlocks, respectively. The promoter for construct 4 was synthesized as an 1,832-bp fragment (Genscript), which was subsequently PCR amplified and cloned into the same hPAH/SV40 pA plasmid as described above by Gibson Assembly. All constructs were cloned into a plasmid containing AAV2 ITRs. All constructs were fully sequenced and verified. Vector genomes were packaged into AAVHSC15, a clade F AAV isolated from human $CD34^+$ human peripheral blood stem cells.[19]

The WT *PAH* cDNA was modified based on individual codon usage, codon context, codon adaption index, and low CpG count relative to the human genome by the COOL codon optimization tool. COOL generated 56 codon-optimized cDNAs. A subset of five cDNAs was selected for screening. The percentage identity was determined in a pairwise manner for cDNA sequences by the Geneious program. cDNA heatmaps and clustering were performed with the pheatmap package in R. Additional codon optimization was performed with Genscript's OptimumGene tool (US patent no. 8,326,547).

Production of AAV Vectors

AAVHSC15 vector stocks were produced by transient triple transfection of HEK293 cells and CsCl gradient sedimentation as previously described,[57] and formulated in a buffer consisting of 5% sorbitol and 0.001% pluronic F-68 in PBS (pH 7.6). Vector preparations were titered by droplet digital PCR (ddPCR), purity of vectors was assessed by 4%–12% sodium dodecyl sulfate (SDS)-acrylamide gel electrophoresis and silver staining (Invitrogen, Carlsbad, CA) and morphological integrity of virions was assessed by transmission electron microscopy of negative-stained rAAV virions at Electron Microscopy Core (UMass Medical School, Worcester, MA). Vector genome titers were determined by ddPCR analysis using the following SV40 primers and probe—forward, 5′-CCAGACATGATAAGATACATTGATGAGTT-3′, reverse, 5′-AGCAATAGCATCACAAATTTCACAA-3′; probe, 5′-AGCATTTTTTTCACTGCATTCTAGTTGTGGTTTGTC-3′—or the following set for the human *PAH* sequences: forward, 5′-GTACTATGTGGCCGAGTCTTT-3′; reverse, 5′-GTATTATCCAGCACCTCGATCC-3′; probe, 5′-ACGATGCCAAGGAGAAGGTGAGAA-3′.

Animal Procedures

Colonies of PKU mice, BTBR-Pah^{enu2}, and their parental strain, BTBR (obtained from Jackson Laboratory, Bar Harbor, ME, USA), were maintained in the animal facility at Homology Medicines, Inc. under standard laboratory conditions (temperature, 20°C –24°C; relative humidity, 50%–60%; 12-h light/12-h dark cycle). Animals were supplied with standard chow (PicoLab 5058, providing approximately 25% of energy as protein and containing 0.97% Phe) and sterile water *ad libitum*. For experiments, 7-week-old adult males were injected with AAV particles into tail veins using a 1-mL syringe with a 28-gauge needle. For Phe monitoring, blood was collected from the facial vein, and serum or plasma was extracted and evaluated for Phe and Tyr levels. All procedures were approved by the Institutional Animal Care and Use Committee at Homology Medicines, Inc. No changes in survival were observed in mice treated with AAVHSC15 when compared to control untreated mice.

Determination of Phe and Tyr by RapidFire-MS

Blood samples were taken as described above and analyzed using a RapidFire 300/Sciex API 4000 QqQ mass spectrometer (MS). Standard curve and internal standards were 2 mmol/L $^{13}C_6$-Phe and 0.2 mmol/L $^{13}C_9$-Tyr in water. The RapidFire-MS protocol, as developed, provided a linear signal up to 20 μmol/L with a lower limit of quantitation approximately 10 nmol/L. Prior to analysis, samples were diluted 250-fold in high-pressure liquid chromatography (HPLC) water. Following analysis on the Rapidfire-MS, the calculated peak areas of the eight $^{13}C_9$-Tyr and $^{13}C_6$-Phe concentrations were plotted versus the internal standard concentrations. The linear fit for the eight data points (including the blank where only background signal should be detected) had an R^2 correlation value of 0.97 or higher. The average peak area of the eight injections for each sample for both Phe and Tyr fell within the linear range of the internal standard injections and had a CV of 15% or better, or was retested. The stable isotope standard curves for $^{13}C_9$-Tyr and $^{13}C_6$-Phe were used to calculate the unknown concentrations of Phe and Tyr in each specimen.

Determination of Vector Genome Copy Numbers in Liver Samples

rAAV genomes were quantified in 1-μg samples of genomic DNA extracted from mouse livers using the QIAamp DNA mini kit for quantitative detection of vector genome copies by TaqMan probes

(Applied Biosystems, Foster City, CA, USA) with a single-copy endogenous glyceraldehyde 3-phosphate dehydrogenase (GAPDH) gene as the diploid cell number reference. A TaqMan real-time PCR kit was run with primer sets that amplified regions of the hPAH or SV40. Briefly, isolated DNA was tested for purity and concentration by spectrophotometry. PCR reactions were performed in 20 μL of final volume using the 2× Universal TaqMan master mix (Applied Biosystems, Foster City, CA, USA) supplemented with 100 nM each of sense and antisense primer, and 2 μL of diluted template DNA (either plasmid standard or extracted sample DNA according to the manufacturer's instructions). All samples and controls were run in three replicates of 20 μL of reactions in alternate rows of a 384-well optical plate. The PCR profile contained an initial denaturation step at 95°C for 10 min followed by 40 cycles of denaturation at 95°C for 15 s and annealing or extension at 60°C for 1 min. Data analysis was performed using Applied Biosystems QuantStudio software v1.3. The sensitivity of the assay was 10 copies/150 ng of cellular DNA. Samples were evaluated for vector biodistribution using the following primers and probes: SV40, forward, 5′-CCAGACATG ATAAGATACATTGATGAGTT-3′, reverse, 5′-AGCAATAGCATC ACAAATTTCACAA-3′, probe, 5′-AGCATTTTTTTCACTGCAT TCTAGTTGTGGTTTGTC-3′; human PAH, forward, 5′-GTACT ATGTGGCCGAGTCTTT-3′, reverse, 5′-GTATTATCCAGCACCT CGATCC-3′, probe, 5′-ACGATGCCAAGGAGAAGGTGAGAA-3′.

Determination of mRNA levels by qRT-PCR

A QIAGEN RNeasy Plus mini kit was used to extract mRNA from mouse livers following the manufacturer's protocol. RNA concentrations were determined by NanoDrop and subsequently treated with DNase. Samples with a spectrophotometric ratio of absorbance at 260 and 280 nm between 1.8 and 2.0 were considered acceptable for use, diluted to 100 ng/μL, and reverse transcribed to cDNA.

mRNA levels were measured by qRT-PCR using an Applied Biosystems QuantStudio 6 Flex system (Thermo Fisher Scientific). Briefly, mRNA levels for PAH and the reference gene, hypoxanthine guanine phosphoribosyl transferase (HPRT), were determined by qPCR using specific sets of primers and probes as follows: human PAH, forward, 5′-GTACTATGTGGCCGAGTCTTT-3′, reverse, 5′-GTATTATCCAGCACCTCGATCC-3′, probe, 5′-ACGATGCCAAG GAGAAGGTGAGAA-3′; HPRT, forward, 5′-GTTAAGCAGTAC AGCCCCAAAATG-3′, reverse, 5′-AAATCCAACAAAGTCTGGCC TGTA-3′, probe, 5′-AGCTTGCTGGTAAAAGGACCTCTCGAA GT-3′.

Data were collected in triplicate as Ct (threshold cycle) values, and the ΔΔCt method was applied to calculate *PAH* mRNA levels relative to the levels of the reference gene, HPRT. Results were expressed as ratios of the gene-specific signal to the internal reference signal, yielding a corrected relative value for the gene-specific product in each sample. Samples with Ct values higher than 32 or equivalent to water controls Ct were considered outside the optimal ranges.

Determination of PAH Activity in Liver Samples

The liver PAH enzyme activity analysis was conducted using a research-grade non-good laboratory practice (GLP) method developed at PureHoney Technologies (Billerica, MA, USA). Briefly, approximately 50 mg of liver tissue was homogenized using a Precellys homogenizer. Protein concentration was assessed (Pierce BCA [bicinchoninic acid] protein assay kit) and the homogenate diluted with phosphate-buffered saline to a 1 mg/mL concentration for use in the PAH enzyme assay. The 2× substrate solution (final assay concentration of 200 mM potassium phosphate/150 mM potassium chloride, 400 μg/mL catalase, 300 mM ammonium iron (II) sulfate, 2 mM dithiothreitol, 200 mM [$^{13}C_6$]-Phe, and 200 μM tetrahydrobiopterin in aqueous solution) and 2× enzyme solution (final assay concentration of 200 mM potassium phosphate/150 mM potassium chloride, 400 μg/mL catalase, 300 mM ammonium iron (II) sulfate, 2 mM dithiothreitol, and 400 μg/mL liver extract) were added to a 96-well microplate and incubated at room temperature for a specified time period (during this time period, any PAH present in the liver sample converts Phe to Tyr through oxidation). The enzyme reaction was quenched by the addition of 10 μL of 10% formic acid containing 5 μM [$^{13}C_9$]-Tyr. Samples were then analyzed by the RapidFire liquid chromatography-tandem mass spectrometry (LC-MS/MS) method.

The slope was determined for each individual sample within the linear range, either from 0 to 10 min or from 0 to 15 min. The background for the assay was determined by taking the average of the vehicle control and subtracted from the slope of each individual animal as well as from the control samples.

Determination of 5-HIAA

Mouse brains were homogenized in PBS and vortexed for 15 min. Lysates were spun down at maximum speed for 5 min to clarify the debris, and the supernatant was extracted with a 50:50 mixture of methanol and acetonitrile. Extract was clarified by vortexing at high speed and centrifugation at 16,000 rpm for 15 min. Supernatant was transferred to an amber liquid chromatography vial and diluted with deionized water to prepare for LC-MS/MS injection. 5-HIAA-d5 was used as an internal standard.

SUPPLEMENTAL INFORMATION

Supplemental Information can be found online at https://doi.org/10.1016/j.omtm.2020.03.009.

AUTHOR CONTRIBUTIONS

S.S.A., A.S., J.L.E., and O.L.F. designed research; S.S.A., H.R., M.W., D.F., A.S., S.N.D., N.A., and J.L. performed research; S.S.A., M.L., and L.A.-S. analyzed data; D.L. and T.W. had scientific input; and S.S.A. and O.L.F. wrote the manuscript

CONFLICTS OF INTEREST

All authors are employees or former employees of Homology Medicines, Inc. and hold equity in the company.

ACKNOWLEDGMENTS

We thank Tim Kelly for stimulating discussions, scientific feedback, and helpful interactions. This research was supported by internal funding from Homology Medicines.

REFERENCES

1. Curtius, H.C., Niederwieser, A., Viscontini, M., Leimbacher, W., Wegmann, H., Blehova, B., Rey, F., Schaub, J., and Schmidt, H. (1981). Serotonin and dopamine synthesis in phenylketonuria. Adv. Exp. Med. Biol. *133*, 277–291.
2. Williams, R.A., Mamotte, C.D., and Burnett, J.R. (2008). Phenylketonuria: an inborn error of phenylalanine metabolism. Clin. Biochem. Rev. *29*, 31–41.
3. Blau, N., Hennermann, J.B., Langenbeck, U., and Lichter-Konecki, U. (2011). Diagnosis, classification, and genetics of phenylketonuria and tetrahydrobiopterin (BH4) deficiencies. Mol. Genet. Metab. *104* (*Suppl*), S2–S9.
4. Burgard, P., Rey, F., Rupp, A., Abadie, V., and Rey, J. (1997). Neuropsychologic functions of early treated patients with phenylketonuria, on and off diet: results of a cross-national and cross-sectional study. Pediatr. Res. *41*, 368–374.
5. Oh, H.J., Park, E.S., Kang, S., Jo, I., and Jung, S.C. (2004). Long-term enzymatic and phenotypic correction in the phenylketonuria mouse model by adeno-associated virus vector-mediated gene transfer. Pediatr. Res. *56*, 278–284.
6. Lee, P., Treacy, E.P., Crombez, E., Wasserstein, M., Waber, L., Wolff, J., Wendel, U., Dorenbaum, A., Bebchuk, J., Christ-Schmidt, H., et al.; Sapropterin Research Group (2008). Safety and efficacy of 22 weeks of treatment with sapropterin dihydrochloride in patients with phenylketonuria. Am. J. Med. Genet. A. *146A*, 2851–2859.
7. Ford, S., O'Driscoll, M., and MacDonald, A. (2018). Living with phenylketonuria: lessons from the PKU community. Mol. Genet. Metab. Rep. *17*, 57–63.
8. Shedlovsky, A., McDonald, J.D., Symula, D., and Dove, W.F. (1993). Mouse models of human phenylketonuria. Genetics *134*, 1205–1210.
9. Nagasaki, Y., Matsubara, Y., Takano, H., Fujii, K., Senoo, M., Akanuma, J., Takahashi, K., Kure, S., Hara, M., Kanegae, Y., et al. (1999). Reversal of hypopigmentation in phenylketonuria mice by adenovirus-mediated gene transfer. Pediatr. Res. *45*, 465–473.
10. Mingozzi, F., and High, K.A. (2013). Immune responses to AAV vectors: overcoming barriers to successful gene therapy. Blood *122*, 23–36.
11. Fang, B., Eisensmith, R.C., Li, X.H., Finegold, M.J., Shedlovsky, A., Dove, W., and Woo, S.L. (1994). Gene therapy for phenylketonuria: phenotypic correction in a genetically deficient mouse model by adenovirus-mediated hepatic gene transfer. Gene Ther. *1*, 247–254.
12. Ding, Z., Harding, C.O., Rebuffat, A., Elzaouk, L., Wolff, J.A., and Thöny, B. (2008). Correction of murine PKU following AAV-mediated intramuscular expression of a complete phenylalanine hydroxylating system. Mol. Ther. *16*, 673–681.
13. Harding, C.O., Gillingham, M.B., Hamman, K., Clark, H., Goebel-Daghighi, E., Bird, A., and Koeberl, D.D. (2006). Complete correction of hyperphenylalaninemia following liver-directed, recombinant AAV2/8 vector-mediated gene therapy in murine phenylketonuria. Gene Ther. *13*, 457–462.
14. Yagi, H., Ogura, T., Mizukami, H., Urabe, M., Hamada, H., Yoshikawa, H., Ozawa, K., and Kume, A. (2011). Complete restoration of phenylalanine oxidation in phenylketonuria mouse by a self-complementary adeno-associated virus vector. J. Gene Med. *13*, 114–122.
15. Smith, L.J., Ul-Hasan, T., Carvaines, S.K., Van Vliet, K., Yang, E., Wong, K.K., Jr., Agbandje-McKenna, M., and Chatterjee, S. (2014). Gene transfer properties and structural modeling of human stem cell-derived AAV. Mol. Ther. *22*, 1625–1634.
16. Gu, X.F., Zhang, M., and Chen, R.G. (1995). Phenylketonuria mutations in southern Chinese detected by denaturing gradient gel electrophoresis in exon 7 of PAH gene. J. Inherit. Metab. Dis. *18*, 753–754.
17. Yuan, R., Tsaih, S.W., Petkova, S.B., Marin de Evsikova, C., Xing, S., Marion, M.A., Bogue, M.A., Mills, K.D., Peters, L.L., Bult, C.J., et al. (2009). Aging in inbred strains of mice: study design and interim report on median lifespans and circulating IGF1 levels. Aging Cell *8*, 277–287.
18. Ellsworth, J.L., O'Callaghan, M., Rubin, H., and Seymour, A. (2018). Low seroprevalence of neutralizing antibodies targeting two clade F AAV in humans. Hum. Gene Ther. Clin. Dev. *29*, 60–67.
19. Smith, L.J., Wright, J., Clark, G., Ul-Hasan, T., Jin, X., Fong, A., Chandra, M., St Martin, T., Rubin, H., Knowlton, D., et al. (2018). Stem cell-derived clade F AAVs mediate high-efficiency homologous recombination-based genome editing. Proc. Natl. Acad. Sci. USA *115*, E7379–E7388.
20. Hamman, K.J., Winn, S.R., and Harding, C.O. (2011). Hepatocytes from wild-type or heterozygous donors are equally effective in achieving successful therapeutic liver repopulation in murine phenylketonuria (PKU). Mol. Genet. Metab. *104*, 235–240.
21. Jones, P.A., and Baylin, S.B. (2002). The fundamental role of epigenetic events in cancer. Nat. Rev. Genet. *3*, 415–428.
22. Faust, S.M., Bell, P., Cutler, B.J., Ashley, S.N., Zhu, Y., Rabinowitz, J.E., and Wilson, J.M. (2013). CpG-depleted adeno-associated virus vectors evade immune detection. J. Clin. Invest. *123*, 2994–3001.
23. Takata, M.A., Gonçalves-Carneiro, D., Zang, T.M., Soll, S.J., York, A., Blanco-Melo, D., and Bieniasz, P.D. (2017). CG dinucleotide suppression enables antiviral defence targeting non-self RNA. Nature *550*, 124–127.
24. Yamamoto, S., Yamamoto, T., Kataoka, T., Kuramoto, E., Yano, O., and Tokunaga, T. (1992). Unique palindromic sequences in synthetic oligonucleotides are required to induce IFN [correction of INF] and augment IFN-mediated [correction of INF] natural killer activity. J. Immunol. *148*, 4072–4076.
25. Krieg, A.M., Yi, A.K., Matson, S., Waldschmidt, T.J., Bishop, G.A., Teasdale, R., Koretzky, G.A., and Klinman, D.M. (1995). CpG motifs in bacterial DNA trigger direct B-cell activation. Nature *374*, 546–549.
26. Nair, N., Rincon, M.Y., Evens, H., Sarcar, S., Dastidar, S., Samara-Kuko, E., Ghandeharian, O., Man Viecelli, H., Thöny, B., De Bleser, P., et al. (2014). Computationally designed liver-specific transcriptional modules and hyperactive factor IX improve hepatic gene therapy. Blood *123*, 3195–3199.
27. Höglund, E., Øverli, Ø., and Winberg, S. (2019). Tryptophan metabolic pathways and brain serotonergic activity: a comparative review. Front. Endocrinol. (Lausanne) *10*, 158.
28. Park, J.W., Park, E.S., Choi, E.N., Park, H.Y., and Jung, S.C. (2009). Altered brain gene expression profiles associated with the pathogenesis of phenylketonuria in a mouse model. Clin. Chim. Acta *401*, 90–99.
29. Güttler, F., Azen, C., Guldberg, P., Romstad, A., Hanley, W.B., Levy, H.L., Matalon, R., Rouse, B.M., Trefz, F., de la Cruz, F., and Koch, R. (2003). Impact of the phenylalanine hydroxylase gene on maternal phenylketonuria outcome. Pediatrics *112*, 1530–1533.
30. Davidoff, A.M., Ng, C.Y., Zhou, J., Spence, Y., and Nathwani, A.C. (2003). Sex significantly influences transduction of murine liver by recombinant adeno-associated viral vectors through an androgen-dependent pathway. Blood *102*, 480–488.
31. Scriver, C.R. (2007). The *PAH* gene, phenylketonuria, and a paradigm shift. Hum. Mutat. *28*, 831–845.
32. González, M.J., Polo, M.R., Ripollés, P., Gassió, R., Ormazabal, A., Sierra, C., Roura, R.C., Artuch, R., and Campistol, J. (2018). White matter microstructural damage in early treated phenylketonuric patients. Orphanet J. Rare Dis. *13*, 188.
33. Horrocks, L.A., and Farooqui, A.A. (2004). Docosahexaenoic acid in the diet: its importance in maintenance and restoration of neural membrane function. Prostaglandins Leukot. Essent. Fatty Acids *70*, 361–372.
34. Koletzko, B., Sauerwald, T., Demmelmair, H., Herzog, M., von Schenck, U., Böhles, H., Wendel, U., and Seidel, J. (2007). Dietary long-chain polyunsaturated fatty acid supplementation in infants with phenylketonuria: a randomized controlled trial. J. Inherit. Metab. Dis. *30*, 326–332.
35. Antenor-Dorsey, J.A., Hershey, T., Rutlin, J., Shimony, J.S., McKinstry, R.C., Grange, D.K., Christ, S.E., and White, D.A. (2013). White matter integrity and executive abilities in individuals with phenylketonuria. Mol. Genet. Metab. *109*, 125–131.
36. Brown, C.S., and Lichter-Konecki, U. (2015). Phenylketonuria (PKU): a problem solved? Mol. Genet. Metab. Rep. *6*, 8–12.
37. Woo, S.L., Gillam, S.S., and Woolf, L.I. (1974). The isolation and properties of phenylalanine hydroxylase from human liver. Biochem. J. *139*, 741–749.

38. Nascimento, C., Leandro, J., Lino, P.R., Ramos, L., Almeida, A.J., de Almeida, I.T., and Leandro, P. (2010). Polyol additives modulate the in vitro stability and activity of recombinant human phenylalanine hydroxylase. Appl. Biochem. Biotechnol. *162*, 192–207.

39. Hoskins, J.A., Jack, G., Wade, H.E., Peiris, R.J., Wright, E.C., Starr, D.J., and Stern, J. (1980). Enzymatic control of phenylalanine intake in phenylketonuria. Lancet *1*, 392–394.

40. Scallan, C.D., Jiang, H., Liu, T., Patarroyo-White, S., Sommer, J.M., Zhou, S., Couto, L.B., and Pierce, G.F. (2006). Human immunoglobulin inhibits liver transduction by AAV vectors at low AAV2 neutralizing titers in SCID mice. Blood *107*, 1810–1817.

41. Manno, C.S., Pierce, G.F., Arruda, V.R., Glader, B., Ragni, M., Rasko, J.J., Ozelo, M.C., Hoots, K., Blatt, P., Konkle, B., et al. (2006). Successful transduction of liver in hemophilia by AAV-factor IX and limitations imposed by the host immune response. Nat. Med. *12*, 342–347.

42. Mochizuki, S., Mizukami, H., Ogura, T., Kure, S., Ichinohe, A., Kojima, K., Matsubara, Y., Kobayahi, E., Okada, T., Hoshika, A., et al. (2004). Long-term correction of hyperphenylalaninemia by AAV-mediated gene transfer leads to behavioral recovery in phenylketonuria mice. Gene Ther. *11*, 1081–1086.

43. Sarkissian, C.N., Gámez, A., Wang, L., Charbonneau, M., Fitzpatrick, P., Lemontt, J.F., Zhao, B., Vellard, M., Bell, S.M., Henschell, C., et al. (2008). Preclinical evaluation of multiple species of PEGylated recombinant phenylalanine ammonia lyase for the treatment of phenylketonuria. Proc. Natl. Acad. Sci. USA *105*, 20894–20899.

44. Szypowska, A., Franek, E., Grzeszczak, W., Filipow, W., Zięba, M., Kabicz, P., Więckowska, B., Sykut-Cegielska, J., and Taybert, J. (2018). Medical care of patients with disorders of aromatic amino acid metabolism: a report based on the Polish National Health Fund data records. Pediatr. Endocrinol. Diabetes Metab. *2018*, 118–125.

45. Gao, G.P., Lu, Y., Sun, X., Johnston, J., Calcedo, R., Grant, R., and Wilson, J.M. (2006). High-level transgene expression in nonhuman primate liver with novel adeno-associated virus serotypes containing self-complementary genomes. J. Virol. *80*, 6192–6194.

46. Nathwani, A.C., Gray, J.T., Ng, C.Y., Zhou, J., Spence, Y., Waddington, S.N., Tuddenham, E.G., Kemball-Cook, G., McIntosh, J., Boon-Spijker, M., et al. (2006). Self-complementary adeno-associated virus vectors containing a novel liver-specific human factor IX expression cassette enable highly efficient transduction of murine and nonhuman primate liver. Blood *107*, 2653–2661.

47. McCarty, D.M. (2008). Self-complementary AAV vectors; advances and applications. Mol. Ther. *16*, 1648–1656.

48. Wu, Z., Sun, J., Zhang, T., Yin, C., Yin, F., Van Dyke, T., Samulski, R.J., and Monahan, P.E. (2008). Optimization of self-complementary AAV vectors for liver-directed expression results in sustained correction of hemophilia B at low vector dose. Mol. Ther. *16*, 280–289.

49. Pohar, J., Kužnik Krajnik, A., Jerala, R., and Benčina, M. (2015). Minimal sequence requirements for oligodeoxyribonucleotides activating human TLR9. J. Immunol. *194*, 3901–3908.

50. Bauer, M., Heeg, K., Wagner, H., and Lipford, G.B. (1999). DNA activates human immune cells through a CpG sequence-dependent manner. Immunology *97*, 699–705.

51. Pacak, C.A., Sakai, Y., Thattaliyath, B.D., Mah, C.S., and Byrne, B.J. (2008). Tissue specific promoters improve specificity of AAV9 mediated transgene expression following intra-vascular gene delivery in neonatal mice. Genet. Vaccines Ther. *6*, 13.

52. Colella, P., Sellier, P., Costa Verdera, H., Puzzo, F., van Wittenberghe, L., Guerchet, N., Daniele, N., Gjata, B., Marmier, S., Charles, S., et al. (2018). AAV gene transfer with tandem promoter design prevents anti-transgene immunity and provides persistent efficacy in neonate Pompe mice. Mol. Ther. Methods Clin. Dev. *12*, 85–101.

53. Kwon, J.H., Lee, Y.M., Cho, J.H., Kim, G.Y., Anduaga, J., Starost, M.F., Mansfield, B.C., and Chou, J.Y. (2017). Liver-directed gene therapy for murine glycogen storage disease type Ib. Hum. Mol. Genet. *26*, 4395–4405.

54. Sarukhan, A., Camugli, S., Gjata, B., von Boehmer, H., Danos, O., and Jooss, K. (2001). Successful interference with cellular immune responses to immunogenic proteins encoded by recombinant viral vectors. J. Virol. *75*, 269–277.

55. Chuah, M.K., Petrus, I., De Bleser, P., Le Guiner, C., Gernoux, G., Adjali, O., Nair, N., Willems, J., Evens, H., Rincon, M.Y., et al. (2014). Liver-specific transcriptional modules identified by genome-wide in silico analysis enable efficient gene therapy in mice and non-human primates. Mol. Ther. *22*, 1605–1613.

56. Picanço-Castro, V., Russo-Carbolante, E.M., Fontes, A.M., Fernandes, A.C., and Covas, D.T. (2008). An enhancer/promoter combination strengthens the expression of blood-coagulation factor VIII in non-viral expression vectors. Genet. Mol. Res. *7*, 314–325.

57. Matsushita, T., Elliger, S., Elliger, C., Podsakoff, G., Villarreal, L., Kurtzman, G.J., Iwaki, Y., and Colosi, P. (1998). Adeno-associated virus vectors can be efficiently produced without helper virus. Gene Ther. *5*, 938–945.

OMTM, Volume *17*

Supplemental Information

Sustained Correction of a Murine Model of Phenylketonuria following a Single Intravenous Administration of AAVHSC15-PAH

Seemin S. Ahmed, Hillard Rubin, Minglun Wang, Deiby Faulkner, Arnold Sengooba, Serena N. Dollive, Nancy Avila, Jeff L. Ellsworth, Diana Lamppu, Maria Lobikin, Jason Lotterhand, Laura Adamson-Small, Teresa Wright, Albert Seymour, and Omar L. Francone

Supplemental Figure 1

A.

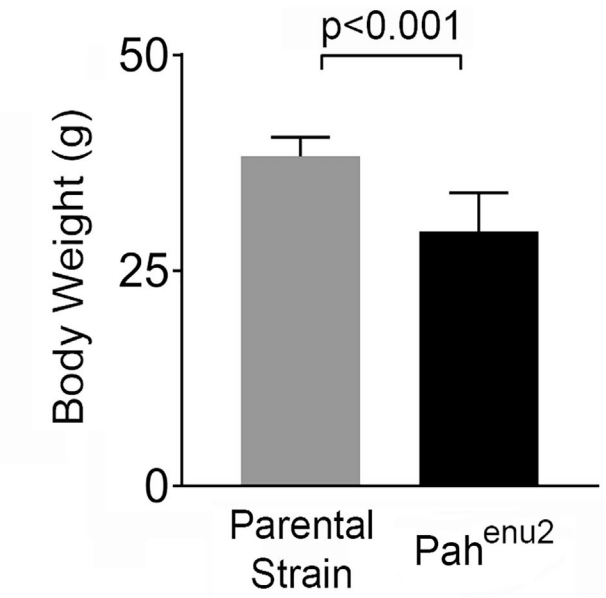

B.

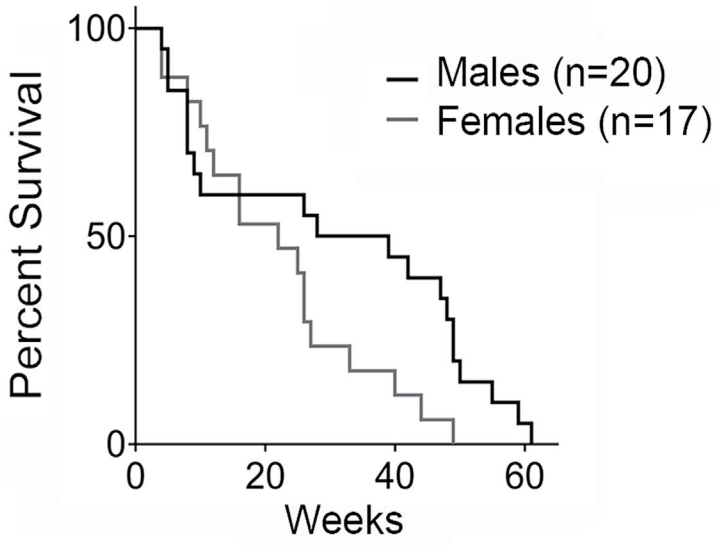

Supplemental Figure 2

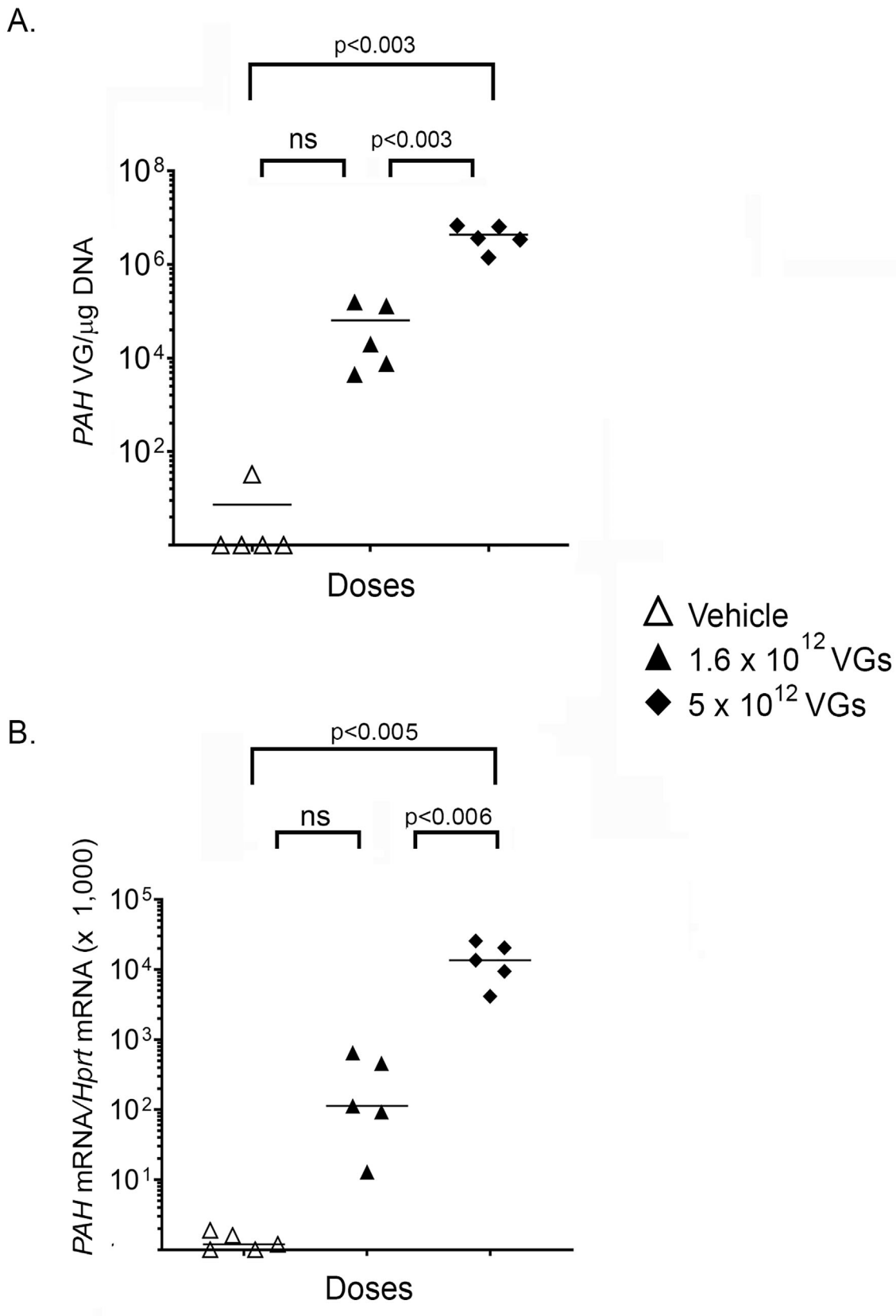

Supplemental Figure 1. Comparison of the Pah^{enu2} mouse and the wild type (WT) mouse phenotypes. A) Comparison of total body weight between Pah^{enu2} mice and WT mice. Data are represented as mean ± Sd; $p<0.001$. B) Survival curve for the Pah^{enu2} male and female mice fed a normal chow diet.

Supplemental Figure 2. Liver vgs and *PAH* mRNA levels following administration of AAVHSC15-CBA-PAH. A) Vector genomes were determined as described under Materials and Methods and expressed as ratio of ug of DNA. B) Human *PAH* mRNA and murine *Hprt* mRNA levels were determined as described under Materials and Methods. Statistical significance was determined by ANOVA.